Quantum Interference in Double Ionization and Fragmentation of C_6H_6 in Intense Laser Fields

V. R. Bhardwaj, D. M. Rayner, D. M. Villeneuve, and P. B. Corkum
National Research Council, 100 Sussex Drive, Ottawa, Ontario, Canada K1A 0R6
(Received 18 July 2001; published 30 November 2001)

During tunnel ionization of atoms or molecules by strong laser fields, the electron acquires a transverse velocity which is characteristic of the ionization process. Ellipticity measurements identify nonsequential double ionization as due to recollision in C_6H_6 and simultaneously measure the transverse velocity distribution of the electron wave packet. We observe signatures of quantum interference of different tunneling trajectories and find identical dependence of nonsequential double ionization and fragmentation of C_6H_6 on the ellipticity of the laser polarization. This identifies electron recollision as the dominant source of fragmentation at 1.4 μm.

DOI: 10.1103/PhysRevLett.87.253003 PACS numbers: 33.80.Rv

Ionization of atoms in intense laser fields is now well understood. This was largely achieved by combining theoretical simulations which use single active electron ionization models [1] with careful measurements of intensity dependence of the ion yield [2,3] and through electron spectroscopy [4,5]. High charge states can be reached by two mechanisms. Electrons can be removed (i) sequentially in single electron steps or (ii) nonsequentially due to the primary electron inelastically rescattering from the ion during a recollision [6,7]. In the second mechanism, following ionization the primary electron oscillates in the electric field of the laser. It can subsequently revisit the ionic core with sufficient energy to excite or further ionize it.

If recollision occurs in atoms then the analogous process must occur in molecules. The purpose of this paper is threefold. First, we clearly identify nonsequential double ionization in C_6H_6 by studying the dependence of double ionization on the ellipticity of the laser polarization. This approach is a standard procedure for identifying recollision in atoms [8–10].

Second, we show that both fragmentation and double ionization have identical ellipticity dependence. At intensities of 10^{14} W/cm^2, for 1.4 μm light we show that all fragmentation is due to recollision. Fragmentation in C_6H_6 can be switched on or off with small changes in the ellipticity of the laser polarization.

Third, we used electron recollision to identify quantum interference in the first ionization step. The transverse velocity ($v_\perp$) of the electron is a characteristic signature of the intrinsic quantum mechanical nature of strong field ionization and is sensitive to quantum interference. For atoms, the transverse velocity has a Gaussian distribution with $1/e$ width given by $\Delta v_\perp = (E/\sqrt{2I_p})^{1/2}$ [11,12], where I_p is the ionization potential of the atom and E is the electric field amplitude. We measured the transverse velocity distribution by studying the dependence of double ionization on the laser polarization [8]. We show that the overall width of the transverse velocity distribution is similar to that for atoms. However, interference between different electron trajectories during the tunneling process results in a structure in the polarization dependence of ion yields that is not observed for rare gas atoms.

Only a few experiments have studied double ionization of molecules. All were performed at 800 nm [13–17]. At 800 nm, for molecules with relatively low values of I_p ($<$10 eV), the recollision energy is low and the ionization process is complex due to competition between multiphoton ionization and tunnel ionization. We choose 1.4 μm light because (1) at typical intensities of 10^{14} W/cm^2 the ponderomotive potential $U_p > I_p$ placing us in a purely tunneling regime [18]; (2) typical electron recollision energy at these intensities is on the order of $3.2U_p \approx 55$ eV, well above the ionization potential of $C_6H_6^+$ (16.7 eV); (3) at longer wavelengths recollision is more sensitive to ellipticity, allowing us to measure the transverse spread more easily.

Experiments are carried out in a single stage time-of-flight (TOF) mass spectrometer, which is 30 cm long. Differential pumping allows the TOF source chamber to be operated up to 10^{-5} Torr, while maintaining the flight chamber under high vacuum. The number density in the interaction volume is low enough to avoid space charge effects. A 500 μm slit at the entrance to the drift region of the TOF spectrometer collects the ions produced in the focal volume with a Rayleigh range of $\sim$500 μm.

An optical parametric amplifier, operated at a repetition rate of 500 Hz, pumped by 50 fs, 750 μJ, 800 nm pulses, produces orthogonally polarized signal and idler wavelengths at 1400 and 1850 nm. Using a broad bandwidth cube polarizer we select the signal wavelength at 1400 nm with output energy of 75 μJ. The pulse duration is measured to be 70 fs using a second harmonic FROG (frequency resolved optical gating). A Berek variable wave plate is used in the $\lambda/4$ configuration to change the ellipticity of the laser polarization.

A 22-cm-long focal length lens focuses the 1400 nm pulses to a spot size of about 15 $\pm$ 3 μm inside the vacuum chamber with a base pressure of 10^{-7} Torr. The microchannel plate detector is operated in an ion-counting

mode in conjunction with a multichannel scaler. We obtain ion yields by integrating the appropriate peaks. To analyze the ellipticity of the laser polarization we use a broad bandwidth polarizer after the variable wave plate. Using a photodiode we determine the maximum and minimum laser intensities with 360° rotation of the polarizer. The ellipticity, defined as the ratio of the two electric field components ($\varepsilon = E_y/E_x$), is less than 0.02 for linear polarization. A part of the input light is reflected onto a fast photodiode to monitor the intensity. Intensity calibration is obtained by measuring the saturation intensity of Xe^+ and comparing it with that calculated by the Ammosov-Delone-Krainov model [11].

Figure 1 shows the ellipticity dependence of the $C_6H_6^{2+}$ signal and the sum of the most important fragments. (Although the peak field of the laser drops with the ellipticity, this decrease is very small for small ellipticities. We show in Fig. 2 that the small decrease in field has negligible effect on the ratio.) Individually every fragment shows the same ellipticity dependence as the double ionization. We observe $C_4H_n^+$ ($n = 2, 3, 4$) and $C_5H_n^+$ ($n = 2, 3$) fragmentation channels with $C_4H_4^+$ as the most dominant channel. Also shown for comparison purposes is the ellipticity dependence of Xe^{2+} obtained at 10^{14} W/cm^2.

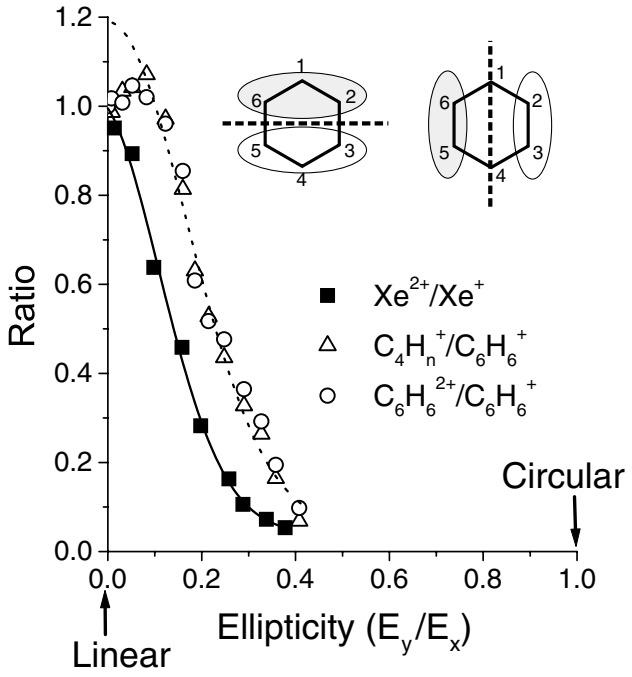

FIG. 1. Measured ratios of doubly to singly charged C_6H_6 and fragment to singly charged C_6H_6 plotted as a function of ellipticity of the laser polarization at an intensity of 7×10^{13} W/cm^2. Also shown is the ratio of Xe^{2+}/Xe^+ obtained at an intensity of 10^{14} W/cm^2. The solid and dotted curves show the best-fit Gaussian distributions to the experimental data. The data have been normalized to unity at linear polarization. Also shown as an inset is the top view of the highest occupied molecular orbitals in C_6H_6. The shaded regions of the orbitals indicate the opposite phase of the wave function upon reflection.

The solid curve shows the best-fit Gaussian distribution to the experimental data of Xe. The width of the Gaussian distribution is governed by the ionization potential and the laser intensity [11]. The half width of the Xe distribution is consistent with the calculated values from the tunneling model (a width of ~0.16 translates to a measured transverse velocity distribution of 6.4 Å/fs [8] while the calculated distribution is 7 Å/fs [12]). The transverse distribution is estimated by assuming a small cross section and ignoring Coulomb focusing [19].

The contribution of Coulomb focusing can be estimated by comparing the transverse energy the electron acquires due to the perpendicular component of the electric field and due to the scattering it undergoes. For an ellipticity of $\varepsilon \sim 0.1$, the perpendicular component of the electric field typically displaces an electron laterally by ~10 Å, which corresponds to an energy of 0.3 eV. At an impact parameter of 10 Å, 50 eV electrons undergo a deviation of 1.7° due to scattering, which corresponds to a transverse energy of 0.043 eV. Coulomb focusing is insignificant for $\varepsilon \gtrsim 0.1$, while it plays a significant role for $\varepsilon \lesssim 0.05$.

The transverse velocity distribution of the electron, produced by ionization of C_6H_6, is derived from the experimental data shown in Fig. 1. A Gaussian fit to the measured data (dotted curve) deviates significantly for $\varepsilon < 0.1$. However, its half width at half maximum of ~0.25 corresponds to a measured transverse velocity of 5.15 Å/fs. An atom with the same ionization potential will have a transverse spread of 5 Å/fs. Both double ionization and fragmentation have the same ellipticity dependence. So, if double ionization is due to recollision, then fragmentation must also be due to recollision. At the intensity of this measurement (~10^{14} W/cm^2) and at all

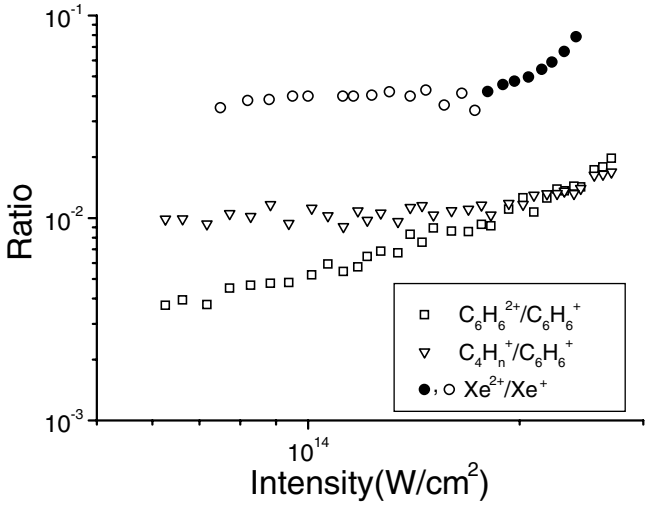

FIG. 2. The ratios of $C_6H_6^{2+}/C_6H_6^+$ and $C_4H_n^+/C_6H_6^+$ plotted as a function of laser intensity for linearly polarized light. Also shown is the ratio of Xe^{2+}/Xe^+. The solid data points represent the transition from nonsequential to sequential double ionization in Xe.

intensities less than this, there is no fragmentation without recollision.

In atoms, the probability of nonsequential double ionization is always maximum for linear polarization and falls off rapidly with the ellipticity of the laser polarization. However, in C_6H_6, both nonsequential double ionization and fragmentation are maximum at an ellipticity of $\varepsilon \sim 0.1$. We now show that this effect is due to the destructive interference between the two components of the wave function in the highest occupied molecular orbital.

The highest occupied molecular orbitals in C_6H_6 are doubly degenerate π orbitals. They both have two nodal planes, one is the plane of the molecule and the other is perpendicular to this plane. A representation of the two degenerate highest occupied molecular orbitals is shown in Fig. 1. The dashed lines indicate nodal planes perpendicular to the molecular plane.

For simplicity, consider C_6H_6 with its plane perpendicular to the laser polarization. When viewed in three dimensions, a saddlelike structure of the potential surface is created by the ionic and laser fields. The saddle point is at a distance of a few angstroms from the ionic core. For tunnel ionization the electron must pass through this restricted region of the saddle. The symmetry of the wave function should be preserved in the saddle region. Electrons from either side of the node travel equal distances to the center of the saddle region, however, with opposite phases. Therefore they interfere destructively.

The momentum distribution of the electrons $\Phi(p)$ in the transverse dimensions is given by the Fourier transform of the spatial wave function $\Psi(r)$ in the saddle region, $\Phi(p) = \int_{-\infty}^{\infty} \Psi(r) e^{-ipr}\, dr$. After it leaves the saddle region and before it returns to the vicinity of the ion, transverse distribution of the electron cannot be changed by linearly polarized light.

For an asymmetric wave function, $\Phi(0) = 0$. Since there are no electrons with zero transverse momentum, none return to the ion in linearly polarized light. This can be understood in terms of destructive interference of the components of the electron wave function after departing the saddle region. Because of destructive interference, there are never any electrons on axis, so there must be a minimum in the nonsequential double ionization/fragmentation.

In elliptically polarized light, the transverse field component compensates for the initial momentum, forcing some of the electrons to return to the ionic core, increasing the double ionization/fragmentation probability. However, in near circularly polarized light, the transverse field imparts so much momentum that the electrons far overshoot the ionic core and the probability of double ionization/fragmentation drops to zero.

We have described what we would expect for a C_6H_6 molecule aligned perpendicular to the laser polarization. However, our experiments are performed with randomly oriented molecules. Let us now consider two other orientations. (a) If the laser field is in the molecular plane of C_6H_6 but with polarization parallel to the nodal plane (dashed line in Fig. 1), the argument presented above applies. Therefore we expect a minimum in double ionization/fragmentation probability for linearly polarized light. (b) Since the molecular plane is itself a nodal plane, we again expect a minimum for linearly polarized light, when the laser polarization is perpendicular to the nodal plane (dashed line in Fig. 1).

Any other orientations result in incomplete interference. So, when one considers an ensemble of randomly oriented C_6H_6 molecules, interference effects result in a local minima of nonsequential double ionization/fragmentation signal for linear polarization, as observed in Fig. 1. Such interference effects were first proposed to explain suppressed ionization in molecules [20]. Suppressed ionization was observed in C_6H_6 [13].

Figure 2 shows the ratio of a doubly charged molecular and a singly charged $C_4H_n^+$ fragment to singly charged molecular ions as a function of laser intensity. Also plotted as a reference is the ratio of Xe^{2+}/Xe^{+}. The Xe curve is typical for what is observed for atoms. There is a plateau, which corresponds to nonsequential ionization, while the region where the ratio increases with intensity corresponds to sequential ionization. At 10^{14} W/cm^2 and 1400 nm, 4% of all single ionization events in Xe lead to double ionization.

The plateau of double ionization in C_6H_6 is less distinct compared to Xe. The probability that single ionization will lead to fragmentation is approximately constant over the intensity range that we observed. At 10^{14} W/cm^2, 0.5% of single ionization events leads to double ionization while 1% leads to the dominant fragmentation channel $C_4H_n^+$ ($n = 2, 3, 4$). The sum of all other fragments corresponds to a probability of 0.1%.

In high ionization potential atoms, recollision is assumed to create singly and doubly excited states. In He and Ne any excited state other than high lying Rydberg states [21] is field ionized by the remaining portion of the optical pulse [19]. Based on atomic ionization studies, if fragmentation arises from excited electronic states then double ionization is expected to increase with laser intensity at the expense of fragmentation. This is the general trend in Fig. 2.

Figure 3 shows the intensity dependence of singly and doubly charged C_6H_6, along with dominant singly charged fragments $C_4H_n^+$ ($n = 2, 3, 4$). At low intensities, the yield of $C_4H_4^+$ is higher than $C_6H_6^{2+}$. As the intensity increases, $C_6H_6^{2+}$ grows more rapidly than $C_4H_4^+$ (in electron collision experiments with neutral molecules the appearance energies of $C_4H_4^+$ and $C_6H_6^{2+}$ are 13.9 and 26 eV, respectively [22]). Although $C_4H_4^+$ is consistent with expectations from atomic ionization we might expect similar behavior for other less dominant fragments (such as $C_5H_4^+$, $C_4H_2^+$, and $C_4H_3^+$ whose appearance energies are 15.7, 17.5, and 18.5 eV, respectively [22]). However, when we

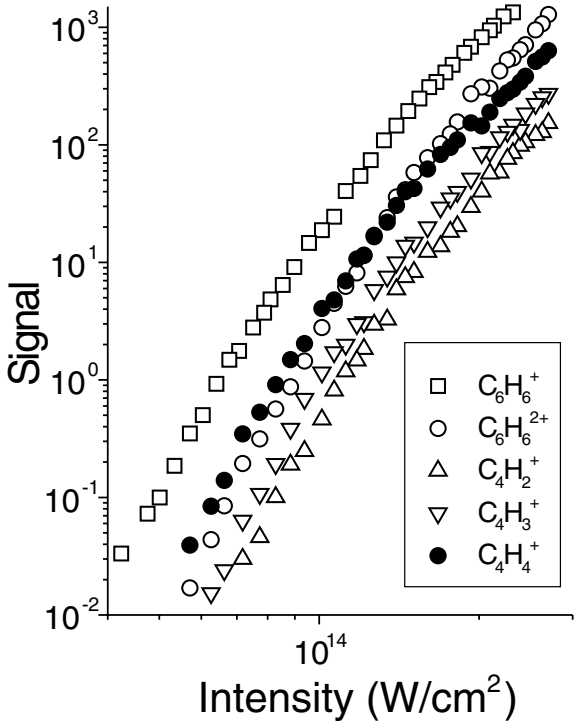

FIG. 3. The intensity dependence of singly and doubly charged C_6H_6, along with dominant singly charged fragments $C_4H_n^+$ ($n = 2, 3, 4$). The yield of $C_6H_6^+$ has been reduced by a factor of 30.

look in detail, we find that most fragmentation channels have the same intensity dependence as in double ionization. Therefore the role and survival of excited states in C_6H_6 is unclear. Experiments where a weak pulse prepares a well-defined excited state of the cation and a strong probe pulse ionizes the excited state will address this problem in the future.

In conclusion, we have measured the transverse velocity distribution of the nascent electron produced by tunnel ionization of randomly oriented C_6H_6. We observe evidence of quantum interference between different tunneling trajectories. If C_6H_6 had been aligned with respect to the laser polarization we predict a deep minimum in double ionization/fragmentation probability for linearly polarized light. Such alignment experiments are technically feasible [23]. Molecular alignment will allow a new class of experiments in which electrons collide with oriented molecules.

[1] K. J. Schafer *et al.,* Phys. Rev. Lett. **70**, 1599 (1993); B. Yang *et al.,* Phys. Rev. Lett. **71**, 3770 (1993).
[2] T. Auguste *et al.,* J. Phys. B **25**, 4181 (1992).
[3] A. Talebpour, C-Y. Chien, and S. L. Chin, J. Phys. B **29**, 5725 (1996); A. Talebpour *et al.,* J. Phys. B **30**, 1721 (1997).
[4] B. Sheehy *et al.,* Phys. Rev. A **58**, 3942 (1998).
[5] R. R. Freeman *et al.,* Phys. Rev. Lett. **59**, 1092 (1987).
[6] P. B. Corkum, Phys. Rev. Lett. **71**, 1994 (1993).
[7] D. N. Fittinghoff *et al.,* Phys. Rev. Lett. **69**, 2642 (1992); B. Walker *et al.,* Phys. Rev. Lett. **73**, 1227 (1994).
[8] P. Dietrich *et al.,* Phys. Rev. A **47**, 2305 (1993).
[9] K. S. Budil *et al.,* Phys. Rev. A **48**, R3437 (1993).
[10] G. G. Paulus *et al.,* Phys. Rev. Lett. **80**, 484 (1998).
[11] M. V. Ammosov, N. B. Delone, and V. P. Krainov, Sov. Phys. JETP **64**, 1191 (1986).
[12] G. L. Yudin and M. Yu. Ivanov, Phys. Rev. A **63**, 033404 (2001).
[13] S. M. Hankin *et al.,* Phys. Rev. Lett. **84**, 5082 (2000).
[14] A. Talebpour, S. Larochelle, and S. L. Chin, J. Phys. B **30**, L245 (1997); A. Talebpour *et al.,* J. Phys. B **33**, 4615 (2001).
[15] C. Cornaggia and Ph. Hering, Phys. Rev. A **62**, 023403 (2000); J. Phys. B **31**, L503 (1998).
[16] C. Guo, M. Li, J. P. Nibarger, and G. N. Gibson, Phys. Rev. A **61**, 033413 (2000); C. Guo and G. N. Gibson, Phys. Rev. A **63**, 040701(R) (2001).
[17] K. W. D. Ledingham *et al.,* J. Phys. Chem. A **102**, 3002 (1998); M. J. DeWitt and R. J. Levis, J. Chem. Phys. **108**, 7045 (1998).
[18] L. V. Keldysh, Sov. Phys. JETP **20**, 1307 (1965).
[19] T. Brabec, M. Yu. Ivanov, and P. B. Corkum, Phys. Rev. A **54**, R2551 (1996); G. L. Yudin and M. Yu. Ivanov, Phys. Rev. A **63**, 033404 (2001); V. R. Bhardwaj *et al.,* Phys. Rev. Lett. **86**, 3522 (2001).
[20] J. Muth-Bohm *et al.,* Chem. Phys. Lett. **337**, 313 (2001); J. Muth-Bohm, A. Becker, and F. H. M. Faisal, Phys. Rev. Lett. **85**, 2280 (2000); F. Grasbon *et al.,* Phys. Rev. A **63**, 041402(R) (2001).
[21] L. D. Noordam *et al.,* Phys. Rev. Lett. **68**, 1496 (1992)
[22] *NIST Chemical Webbook* (http://webbook.nist.gov/chemistry/), edited by W. Mallard, NIST Standard Reference Database Number 69 (NIST, Washington, DC, 2000).
[23] J. J. Larsen *et al.,* Phys. Rev. Lett. **85**, 2470 (2000).